Frequency Trajectory Planning Based Strategy for Improving Frequency Stability of Droop-Controlled Inverter Based Standalone Power Systems

Liansong Xiong, *Member, IEEE,* Lei Liu, Xiaokang Liu, *Member, IEEE,* and Yonghui Liu, *Graduate Student Member, IEEE*

***Abstract*—Inverter-based standalone power systems (ISPSs), with limited inertia/damping, are prone to significant changes in frequency indicators encompassing frequency deviation and rate of change of frequency (RoCoF), which can easily exceed the pertinent relay thresholds and cause power outages. Limited by estimating the disturbance and system inertia/damping deficiency, existing controls cannot ensure system frequency stability. To overcome this issue, a frequency trajectory planning (FTP) based strategy is developed in this manuscript to improve frequency stability of droop-controlled ISPS. This frequency-indicator-oriented control relates system frequency with several pre-defined planning parameters, decoupling from system's disturbances and inertia/damping deficiency that are difficult to evaluate. During normal operation or when the disturbance level is insignificant, the inverter operates in standard droop mode since the system intrinsic inertia/damping features suffice to regulate the frequency. In the event of a large disturbance, an FTP block is triggered by detected frequency indicators, and a marginally safe frequency trajectory is planned according to the requirement of the grid code. In this case, by tracking the planned frequency trajectory, the inverter provides suitable inertia/damping support needed by the system, thereby guaranteeing frequency stability of the ISPS. Finally, simulation and experimental results proved the effectiveness and advancement of the FTP based strategy.**

***Index Terms*—Droop control, frequency stability, frequency deviation, frequency trajectory planning (FTP), rate of change of frequency (RoCoF), standalone power system.**

I. Introduction

With the development of power electronics technology, renewable power generations are progressively adopted in standalone power systems as primary energy sources, as such lowering the generation cost, reducing the environmental pollution and enhancing the electricity supply ability in remote areas [1]–[3]. To interface the renewable source and the AC grid, and to actively support the grid frequency and voltage, the standalone power system dominated by renewable generations exploits a large amount of frequency droop control based inverters. As the initially developed and widely used grid-forming control strategy, the droop control equips inverters with abilities of frequency regulation (via active power control) and voltage regulation (via reactive power control) [4]. Owing to these features, the inverter functions similarly as the synchronous generator (SG) in a large power grid; furthermore, satisfactory power sharing among parallel inverters can be achieved easily [5].

For stable grid operation, the grid code defined limits for various frequency performance indicators, encompassing the frequency deviation, the rate of change of frequency (RoCoF) and so on [3], [6]. However, the frequency stability is more critical in the inverter-based standalone power systems (ISPSs), since the droop-controlled inverter based system lacks sufficient inertia and is prone to severe frequency deviations under random interferences. As a result, frequency related protections can be easily triggered, and a power outage accident is likely to occur [7]. Though efforts have been made to improve the frequency stability of standalone power systems by enhancing the droop control strategy of grid-forming inverters, there are still no effective solutions. Indeed, it is proved in [5] that the low-pass filter (LPF) of droop controller can equivalently provide inertia and suppress RoCoF; however, the inertia support is quite limited due to the fixed LPF bandwidth for filtering the power calculation results. As a result, it has become a mainstream of research to develop alternatives to the droop control.

As a widely concerned solution, the virtual synchronous generator (VSG) control emulates the SG operating characteristics and achieves the grid-forming effect via the inverter control [8]. Since the swing process of SG rotor is simulated and an inertia block with adjustable parameters is introduced into the control structure, the grid-forming inverter based on VSG control can prevent rapid frequency changes during transients, thereby improving the system frequency dynamics. Nevertheless, the VSG control also inherits the complex oscillation characteristics of SG while obtaining inertia features. [9] points out the inevitable oscillation problem when VSGs are operated in parallel, and several works have conducted detailed studies on the influence of inertia parameters in the VSG control on system frequency characteristics [10], [11].

To alleviate the previously mentioned oscillations associated with the VSG control, several adaptive VSG strategies have been proposed. The self-tuning VSG [12], [13] can achieve the optimal performance, yet requiring online solution of the

L. Xiong is with the School of Automation, Nanjing Institute of Technology, Nanjing 211167, China and also with the School of Electrical Engineering, Xi'an Jiaotong University, Xi'an 710049, China, e-mail: xionglian-song@163.com.

L. Liu is with the School of Electrical Engineering, Xi'an Jiaotong University, Xi'an 710049, China, e-mail: LeiLiuxjtu@stu.xjtu.edu.cn.

X. Liu is with the Department of Electronics, Information and Bioengineering, Politecnico di Milano, 20133 Milan, Italy, e-mail: xiaokang.liu@polimi.it.

Y. Liu is with the School of Electrical Engineering, Xi'an Jiaotong University, Xi'an 710049, China, e-mail: liuyonghui@stu.xjtu.edu.cn.

optimal virtual inertia and damping coefficients [14] which cannot be well implemented in embedded controller based inverter systems. The VSG control with alternating moment of inertia [11] exhibits remarkable performance in fast damping of oscillations, however, it does not take the effect of damping factor into consideration [14]. The self-adaptive inertia and damping combination control [14], [15] fully considers the relationship between frequency stability and inertia/damping parameters, and the optimal parameters for achieving lower oscillation amplitude and retaining the stability can be obtained via the optimization method in [16]; however, solving such an optimization problem requires detailed parameters of SGs and line impedances that are mostly unknown. To comply with the grid-tied and the standalone modes simultaneously, [7] proposes a generalized droop control that can function as both a traditional droop control and a VSG control, yet it requires fine-tuned controller parameters and also easily causes large overshoots or oscillations in the grid-tied mode.

The undesired complex oscillations related to the SG model embedded strategies seriously affect the grid frequency stability, and the inverters must stop working for protection when the oscillation amplitude exceeds a certain range. Such oscillations are mainly ascribed to the mismatch of inertia and other parameters in the power system [15]. However, since the system inherent inertia/damping parameters and the random disturbances are unknown, it is difficult to quantitatively evaluate the deficiency of system inertia and damping, and hence impossible to preliminarily design inertia and damping control parameters. As a consequence, grid code requirements on frequency indicators cannot be consistently satisfied with the pertinent control strategy.

To overcome the aforementioned technical challenges, a frequency trajectory planning (FTP) based strategy is developed in this paper, aiming at improving the frequency stability of the ISPS. This strategy is based on frequency performance indicators, and foresees to regulate the inverter i) through the droop-control mode when the system is in normal operation or suffers from insignificant disturbances, as such avoiding the oscillations caused by the use of an SG model, and ii) through an enhanced mode when the influence of a large disturbance cannot be adequately mitigated by the system intrinsic inertia and damping. In the latter case, an auxiliary inertia-damping control module incorporating a proposed FTP block is activated, aiming to achieve the planned frequency trajectory that complies with the requirements on frequency performance indicators, thus substantially improving the system frequency stability.

Compared to the widely used droop control and intensively investigated VSG control, the proposed FTP based strategy is characterized by advantages encompassing the following.

1) The proposed strategy embeds the droop control structure and inherits its merits under small-disturbance conditions. When the frequency deviation and RoCoF are insignificant (viz. the system does not require inertia/damping support), the control system has a simplified equivalent structure suitable for frequency and voltage stabilization and an excellent performance in steady-state power sharing between multiple parallel inverters, yet avoiding the oscillation issue related to VSG model.
2) The enhanced mode avoids the difficulties in estimating system inertia/damping parameters and predicting random disturbances, by directly implementing frequency control based on RoCoF and frequency deviation indicators. To guarantee sufficient inertia and damping for the controlled ISPS, the control system in this mode plans and tracks the frequency trajectory that meets the requirement imposed by pertinent standards.
3) The proposed scheme provides superb compatibility with both the inverter grid-tied mode and the standalone mode. When connected to the utility grid integrated with SGs, inverters with the proposed strategy automatically switch to the grid-friendly droop-mode operation since the utility grid provides the system with required inertia. However, this feature is difficult to be implemented for other inertia controllers since the inertia from inverter needs to match that provided by the system (encompassing contributions from SGs, loads and other converters), otherwise power oscillations can occur in the system [15].

The reminder of this manuscript is outlined as follows. In Sec. II, typical frequency control strategies are analyzed in terms of system frequency response features and main technical challenges. In Sec. III, principles and detailed implementation of the FTP based control strategy are developed. The effectiveness and advancement of the proposed method are verified by simulations and experiments in Sec. IV. Finally, Sec. V draws the main conclusions.

II. Grid-Forming Inverter and Frequency Stability of Standalone Power System

When operating in standalone mode, the inverter along with loads forms the inverter-based standalone power system (ISPS). Generally, the grid-forming inverter actively supports the system voltage and frequency stability via two typical controls, i.e. the droop control and the VSG control.

Dynamic frequency characteristics of the ISPS incorporating grid-forming inverters mainly depend on the inverter control strategy and the load disturbances, which together affect the frequency deviation and RoCoF of the system. When the maxima of these two indicators (i.e. $\Delta f_{\max}$ and $R_{\max}$) exceed the safety thresholds of relevant relays, frequency related protection and control (e.g. under-frequency load shedding and generator disconnection) devices can be triggered, causing power outages. To avoid this, the control strategy of grid-forming inverters should assure the frequency deviation and RoCoF indicators retain within the limits in the event of random disturbances, yielding

$$\begin{cases} |\Delta f|_{\max} \leq F_{\text{std}} \\ |R|_{\max} \leq R_{\text{std}} \end{cases} \tag{1}$$

where F_{std} and R_{std} are thresholds of frequency deviation and RoCoF relays specified by the grid code [17], respectively.

By imposing the constraint in (1), the frequency dynamics and control parameter ranges for the droop and VSG controls are discussed in the following.

A. System Frequency Dynamics under Typical Controls

Without loss of generality, the resistive-inductive load condition is considered as an example, where the active (reactive) power of the droop-controlled inverter is approximately proportional to the system frequency (voltage) [5]. Frequency-droop control in this case can be implemented as in Fig. 1, where D_f and D_q are active and reactive droop coefficients, respectively; P_ref and Q_ref are rated active and reactive powers of the inverter, respectively, and P and Q are active and reactive power outputs by the inverter, respectively.

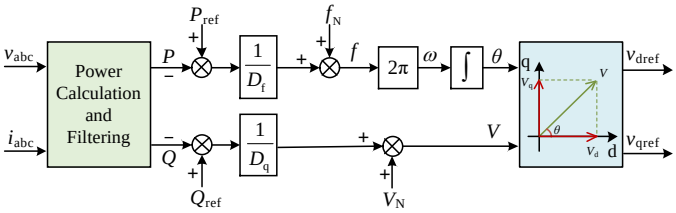

Fig. 1. Frequency-droop control diagram.

The system frequency with inverter droop control yields

$$f = f_\mathrm{N} + \frac{1}{D_\mathrm{f}}\left(P_\mathrm{ref} - P\right) \tag{2}$$

When the ISPS is in steady state, it holds that $P = P_\mathrm{ref}$ and $f = f_\mathrm{N}$. If the load power suddenly increases by P_dis, P can be calculated according to Fig. 1 as

$$P = P_\mathrm{ref} + P_\mathrm{dis} H_\mathrm{LPF}\left(s\right), \tag{3}$$

where $H_\mathrm{LPF}(s)$ is the transfer function of LPF with the time constant T_f and yields

$$H_\mathrm{LPF}\left(s\right) = \frac{1}{1 + T_\mathrm{f} s} \tag{4}$$

Substituting (3) into (2), system frequency during the disturbance can be expressed as

$$f = f_\mathrm{N} - \frac{P_\mathrm{dis}}{D_\mathrm{f}} \frac{1}{1 + T_\mathrm{f} s} \tag{5}$$

The frequency deviation and RoCoF are formulated as

$$\begin{cases} \Delta f = f_\mathrm{N} - f = \dfrac{P_\mathrm{dis}}{D_\mathrm{f}} \dfrac{1}{1 + T_\mathrm{f} s} \\ R = sf = -\dfrac{P_\mathrm{dis}}{D_\mathrm{f}} \dfrac{s}{1 + T_\mathrm{f} s} \end{cases} \tag{6}$$

and their absolute values have the maxima of

$$\begin{cases} \left|\Delta f\right|_\mathrm{max} = \lim\limits_{s \to 0} \left|\Delta f\right| = \dfrac{P_\mathrm{dis}}{D_\mathrm{f}} \\ \left|R\right|_\mathrm{max} = \lim\limits_{s \to \infty} \left|R\right| = \dfrac{P_\mathrm{dis}}{D_\mathrm{f} T_\mathrm{f}} \end{cases} \tag{7}$$

It is seen from (7) that if the droop control is adopted, frequency indicators are greatly affected by the load disturbance (i.e. Δf_max and R_max are proportional to the disturbance level), causing difficulty in retaining system frequency stability. Besides, Δf_max and R_max are influenced by inverter control parameters D_f and T_f, whose allowed value range can be obtained by substituting (7) into (1) as

$$\begin{cases} D_\mathrm{f} \geq \dfrac{P_\mathrm{dis}}{F_\mathrm{std}} \\ T_\mathrm{f} \geq \dfrac{P_\mathrm{dis}}{R_\mathrm{std}} D_\mathrm{f} \end{cases} \tag{8}$$

As previously discussed, T_f is usually small accounting for the power filtering requirements, and the inertia provided by the LPF can be neglected. Accordingly, to equip the ISPS with sufficient inertia and effectively suppress the system RoCoF, the VSG control (see Fig. 2) has been proposed. It is noted that the identical reactive power control in Fig. 1 is always adopted in the VSG control to form the system voltage.

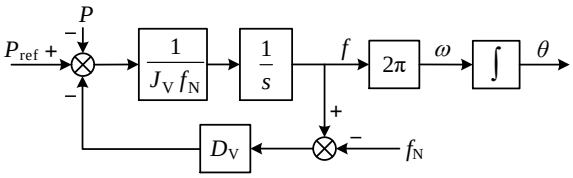

Fig. 2. VSG control diagram.

With the inverter VSG control, the system frequency can be expressed as (with J_V being the virtual inertia coefficient, and D_V the virtual damping coefficient)

$$J_\mathrm{V} f_\mathrm{N} \frac{\mathrm{d}f}{\mathrm{d}t} = P_\mathrm{ref} - P - D_\mathrm{V}\left(f - f_\mathrm{N}\right) \tag{9}$$

Analogous to the previous case, we have

$$f = f_\mathrm{N} - \frac{P_\mathrm{dis}}{D_\mathrm{V}} \left(1 - e^{-\frac{D_\mathrm{V}}{J_\mathrm{V} f_\mathrm{N}} t}\right) \tag{10}$$

Similarly, considering the constraint in (1), value ranges of D_V and J_V can be obtained as

$$\begin{cases} D_\mathrm{V} \geq \dfrac{P_\mathrm{dis}}{F_\mathrm{std}} \\ J_\mathrm{V} \geq \dfrac{P_\mathrm{dis}}{R_\mathrm{std} f_\mathrm{N}} \end{cases} \tag{11}$$

B. Key Technical Challenges

According to (8) and (11), control parameter ranges are related to the disturbance for both control strategies. To properly design these parameters and satisfy the frequency stability requirement, several technical issues need to be resolved:

1) Due to the uncertainty of disturbances, control parameters (D_V, J_V, D_f and T_f) can only be designed according to typical working conditions. Once these parameters are determined, inertia and damping provided by the inverter are constant (and limited). Consequently, the system can hardly maintain frequency stability when large disturbances exceeding the typical operating range occur. In these cases, the frequency deviation and RoCoF indicators easily exceed the safety thresholds, triggering frequency related relays and causing power outages.
2) For ease of discussion, the above analysis only considers the resistive-inductive load without the system inherent

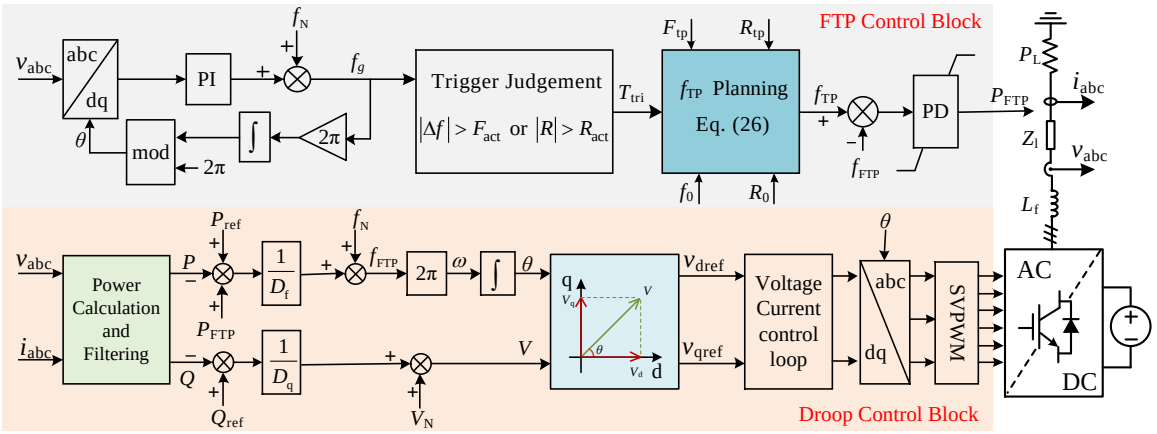

Fig. 3. Studied ISPS with full inverter control diagram incorporating the proposed FTP based strategy.

inertia and damping. In general, the inertia and damping associated with motor loads and converters with the inertia-damping control need to be considered, in order to match the inertia-damping effects provided by the inverter and avoid potential oscillations. However, currently, there is no feasible solution available for estimating the system intrinsic inertia and damping.

3) In addition to the frequency stability, controller parameter design requires to account for several constraints, e.g. fast response, power sharing, working mode (grid-tied or standalone), and inertia/damping shortages under various disturbances, etc. These requirements can be difficult to be satisfied, and may result in contradictions. For example, D_f of the droop control should be small in the grid-tied mode for a fast response, yet significantly large in the standalone mode to ensure sufficient RoCoF suppression under large disturbances.

In response to the above challenges, an FTP based strategy is developed in this manuscript for improving the frequency stability of the ISPS.

III. Frequency Trajectory Planning Control

To ease the analysis, the ISPS (see Fig. 3) is formed by a grid-forming inverter and a resistive-inductive load. With reference to Fig. 3, f_g denotes the grid frequency; f_{TP} is the planned frequency trajectory (within a safety range determined by the critical frequency trajectory f_{cr}); PD is a proportional-differential controller, and P and D parameters adjust the damping and inertia effects provided by the inverter, respectively.

The proposed frequency-indicator-oriented strategy implements frequency control straightforwardly based on frequency deviation and RoCoF indicators, and assures consistently sufficient inertia and damping of the controlled ISPS. To this end, two types of control modes are embedded and switched according to the frequency performance indicators. For relatively small RoCoF and frequency deviation in the ISPS, or when the inverter is connected to the utility grid, the classic droop control is adopted for the control system. Conversely, when the ISPS has significant RoCoF and frequency deviation values (suggesting insufficient inertia and damping effects of the system), an enhanced mode is enabled to limit the frequency indicators within a safety region. In this latter case, the FTP control block generates a reference frequency trajectory within which the frequency deviation and RoCoF satisfy the limits imposed by the grid code, as such assuring the system frequency stability yet avoiding the difficulties in determining control parameters (associated with estimating system inertia/damping, predicting random disturbances, etc.)

A. Critical Frequency Trajectory

With either the droop control or VSG control, from (5) and (10), the standalone power system, affected by the total inertia and damping that originate from the system itself and the inverter, has a frequency response expression encompassing i) a steady-state component f_0 (usually the system rated value f_N) before the disturbance, and ii) a exponentially decayed transient component caused by the disturbance. Specifically, the amplitude F of the transient component depends on the disturbance level and the total system damping, and the attenuation rate σ depends simultaneously on the total inertia and damping. Therefore, the frequency expression of the ISPS after disturbance can be generalized as

$$f = f_0 - F\left(1 - e^{-\sigma t}\right)\text{sign}\left(P_{dis}\right) \tag{12}$$

where, $\text{sign}\left(x\right)$ is a signum function, yielding

$$\text{sign}\left(x\right) = \begin{cases} 1 & x > 0 \\ -1 & x \le 0 \end{cases} \tag{13}$$

To accurately determine the sign of disturbance power in (12), the direction of RoCoF is exploited. If P_{dis} is positive, the disturbance causes system power shortage, frequency drop and negative RoCoF, and vice versa. Hence,

$$\text{sign}\left(P_{dis}\right) = -\text{sign}\left(R\right) \tag{14}$$

Substituting (14) into (12) gives the practical expression of system frequency, namely

$$f = f_0 + F\left(1 - e^{-\sigma t}\right)\text{sign}\left(R\right) \tag{15}$$

General expressions of system frequency indicators are

$$\begin{cases} \Delta f = f_{\mathrm{N}} - f = f_{\mathrm{N}} - f_0 - F\left(1 - e^{-\sigma t}\right)\mathrm{sign}\left(R\right) \\ R = \dfrac{\mathrm{d}f}{\mathrm{d}t} = \sigma F e^{-\sigma t}\mathrm{sign}\left(R\right) \end{cases} \tag{16}$$

Hence, the maxima of absolute frequency indicators are

$$\begin{cases} \left|\Delta f\right|_{\max} = \lim\limits_{t\to\infty}\left|\Delta f\right| = \left|f_{\mathrm{N}} - f_0 - F\mathrm{sign}\left(R\right)\right| \\ \left|R\right|_{\max} = \lim\limits_{t\to 0}\left|R\right| = \sigma F \end{cases} \tag{17}$$

Considering the relative relationships i) between f_0 and f_{N}, and ii) between P_{dis} and 0, the expression of maximum absolute frequency deviation can be reformulated as

$$\left|\Delta f\right|_{\max} = F - \left(f_{\mathrm{N}} - f_0\right)\mathrm{sign}\left(R\right) \tag{18}$$

Analogous to the analysis in Sec. II-A, the frequency indicators in (17) should satisfy (1) to ensure frequency stability. This gives (with F_{cr} and R_{cr} the critical frequency deviation and RoCoF, respectively)

$$\begin{cases} F \le F_{\mathrm{cr}} = F_{\mathrm{std}} + \left(f_{\mathrm{N}} - f_0\right)\mathrm{sign}\left(R\right) \\ \sigma \le \sigma_{\mathrm{cr}} = \frac{R_{\mathrm{std}}}{F_{\mathrm{cr}}} \end{cases} \tag{19}$$

By substituting (19) into (15), practical expression for critical frequency trajectory satisfying the grid code requirement can be obtained as

$$f_{\mathrm{cr}} = f_0 + F_{\mathrm{cr}}\left(1 - e^{-\sigma_{\mathrm{cr}} t}\right)\mathrm{sign}\left(R\right) \tag{20}$$

In passing, it is worth mentioning that all parameters in (20), encompassing i) frequency indicator limits specified by grid codes (F_{std} and R_{std} in F_{cr} and σ_{cr} expressions), and ii) the real-time system frequency (f) and its rate of change (R), can be readily obtained.

According to (20), the safety region of system frequency can be defined (see Fig. 4, where $f_0 = f_{\mathrm{N}}$ is assumed). In the analysis here, disturbance power P_{dis} is assumed to be positive, giving $\mathrm{sign}(P_{\mathrm{dis}}) = 1$ and $\mathrm{sign}(R) = -1$. Denote the critical frequency trajectory determined by (20) as $f_{\mathrm{cr}}^{\mathrm{d}}$, then the frequency stability requirement of system is satisfied when the frequency trajectory f is located between f_{N} and $f_{\mathrm{cr}}^{\mathrm{d}}$ ($f_{\mathrm{cr}}^{\mathrm{d}} < f < f_{\mathrm{N}}$), and vice versa. Hence, the safe operation range of system frequency is the region enclosed by two critical frequency trajectories ($f_{\mathrm{cr}}^{\mathrm{d}} \le f \le f_{\mathrm{cr}}^{\mathrm{u}}$), where $f_{\mathrm{cr}}^{\mathrm{u}}$ is the critical trajectory for negative disturbance power, i.e. when $\mathrm{sign}(R) = 1$.

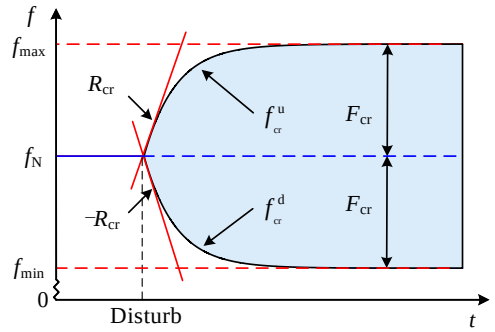

Fig. 4. Frequency safe operation region.

Since the safe operation region of system frequency trajectory can be clearly defined, the target of frequency control is switched from designing the inertia-damping control and its parameters to assuring the frequency trajectory to be limited within the allowable region defined in Fig. 4. To this end, under small disturbance conditions (viz. RoCoF and frequency deviation are both within the safety region), the system can perform frequency control according to the classic droop control; under large disturbance conditions, the system frequency is regulated according to a well planned frequency trajectory, which has sufficient safety margin w.r.t. the critical trajectory determined by (20).

B. Derivation of Planned Frequency Trajectory

Due to the inevitable difference between the actual frequency trajectory and the planned one during the control process, and due also to the time delay related to frequency detection and FTP block triggering, the system frequency may exceed the safety region and trigger frequency related relays if the critical frequency trajectory (20) determined by F_{cr} and R_{cr} is directly used as the control target.

To reliably ensure the frequency stability, enough safety margins F_{mar} and R_{mar} are necessary when planning the frequency evolution trajectory. Therefore, the planned maximum frequency deviation F_{tp} and maximum RoCoF R_{tp} should be

$$\begin{cases} F_{\mathrm{tp}} = F_{\mathrm{std}} - F_{\mathrm{mar}} \\ R_{\mathrm{tp}} = R_{\mathrm{std}} - R_{\mathrm{mar}} \end{cases} \tag{21}$$

To simultaneously guarantee the frequency quality (allowing short-term quality degradation under extreme conditions), F_{tp} and R_{tp} should ensure the frequency quality requirement of the grid code at least. Namely, within the planned frequency trajectory determined by F_{tp} and R_{tp}, the frequency satisfies the quality standard, and the power system operation is satisfactorily efficient. For simplicity, F_{tp} and R_{tp} can be directly determined based on the frequency quality requirement.

Assuming that the FTP control block is triggered at time t_0, the planned frequency trajectory f_{TP} can be expressed on the basis of (15) and the above parameters as (with f_0 and R_0 the actual system frequency and RoCoF values at t_0, respectively)

$$f_{\mathrm{TP}} = f_0 + F\left(1 - e^{-\sigma\left(t - t_0\right)}\right)\mathrm{sign}\left(R_0\right) \tag{22}$$

Parameters in (22) can be determined according to the initial and final value conditions, namely a) at the triggering time, f_{TP} is consistent with the actual system frequency, and its RoCoF equals the planned value R_{tp}; b) the steady-state frequency deviation of f_{TP} should be the planned value F_{tp}. Hence,

$$\begin{cases} \left|\Delta f_{\mathrm{TP}}\right|_{\max} = \lim\limits_{t\to\infty}\left|\Delta f_{\mathrm{TP}}\right| = \left|f_{\mathrm{N}} - f_0 - F\mathrm{sign}\left(R_0\right)\right| = F_{\mathrm{tp}} \\ \left|R_{\mathrm{TP}}\right|_{\max} = \lim\limits_{t\to t_0}\left|R_{\mathrm{TP}}\right| = \sigma F = R_{\mathrm{tp}} \end{cases} \tag{23}$$

By considering (18), (23) can be simplified as

$$\begin{cases} F - \left(f_{\mathrm{N}} - f_0\right)\mathrm{sign}\left(R_0\right) = F_{\mathrm{tp}} \\ \sigma F = R_{\mathrm{tp}} \end{cases} \tag{24}$$

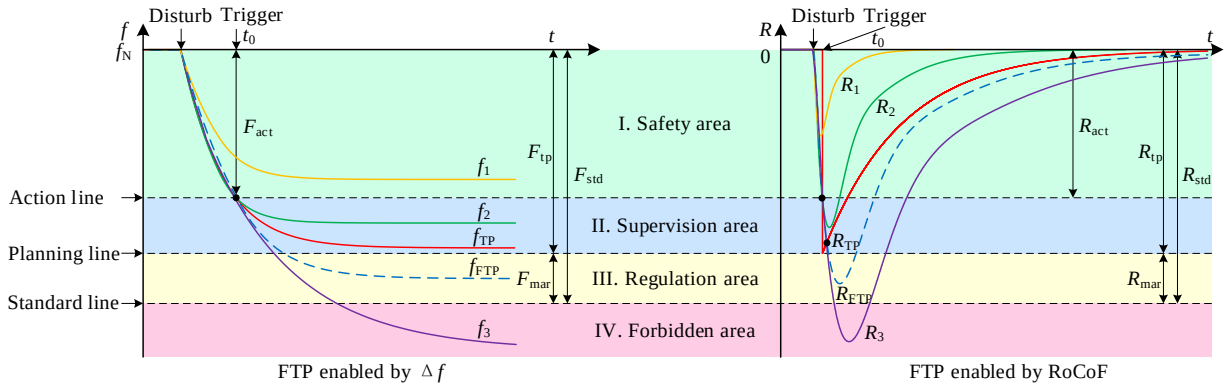

Fig. 5. Frequency trajectory partition. f_{FTP} and R_{FTP} are actual frequency and RoCoF trajectories of the power system under FTP control.

$$f_{\mathrm{TP}}=\begin{cases} f_{\mathrm{N}}+F_{\mathrm{tp}}-(f_{\mathrm{N}}-f_0+F_{\mathrm{tp}})\,e^{-\frac{R_{\mathrm{tp}}}{F_{\mathrm{tp}}+f_{\mathrm{N}}-f_0}(t-t_0)} & \mathrm{sign}\,(R_0)=1 \\ f_{\mathrm{N}}-F_{\mathrm{tp}}-(f_{\mathrm{N}}-f_0-F_{\mathrm{tp}})\,e^{-\frac{R_{\mathrm{tp}}}{F_{\mathrm{tp}}-f_{\mathrm{N}}+f_0}(t-t_0)} & \mathrm{sign}\,(R_0)=-1 \end{cases} \tag{26}$$

Solution to (24) gives the relevant parameters in (22) as

$$\begin{cases} F=F_{\mathrm{tp}}+(f_{\mathrm{N}}-f_0)\,\mathrm{sign}\,(R_0) \\ \sigma=\dfrac{R_{\mathrm{tp}}}{F}=\dfrac{R_{\mathrm{tp}}}{F_{\mathrm{tp}}+(f_{\mathrm{N}}-f_0)\,\mathrm{sign}\,(R_0)} \end{cases} \tag{25}$$

By substituting (25) into (22), expression of the planned frequency trajectory f_{TP} can be obtained as (26) shown at the top of this page. Its pertinent RoCoF trajectory R_{TP} writes

$$R_{\mathrm{TP}}=\frac{\mathrm{d}f_{\mathrm{TP}}}{\mathrm{d}t}=R_{\mathrm{tp}}e^{-\frac{R_{\mathrm{tp}}}{F_{\mathrm{tp}}+(f_{\mathrm{N}}-f_0)\,\mathrm{sign}(R_0)}(t-t_0)}\cdot\mathrm{sign}\,(R_0) \tag{27}$$

Frequency trajectory in (26) can be preliminarily planned, since the involved parameters encompass only i) the planned maximum frequency deviation/RoCoF values F_{tp} and R_{tp}, and ii) the grid frequency information (f_0, R_0) that can be directly measured by the phase-locked loop (PLL). Based on the parameter design method in [18], the PLL can be fine-tuned to effectively restrain the noise disturbances and guarantee the transient stability. Therefore, technical challenges previously discussed in Sec. II-B are effectively avoided by resorting to the more practical FTP based scheme here proposed.

C. Frequency Trajectory Partition

Due to the inertia effect, the system frequency cannot be changed instantaneously. Hence, the FTP control should be enabled before the frequency deviation and RoCoF reach their planned values F_{tp} and R_{tp}. Considering the frequency deviation and RoCoF action values F_{act} and R_{act} at which the trajectory planning block is enabled, the pertinent trigger signal T_{tri} can be expressed as (see Fig. 3, where $T_{\mathrm{tri}}=1$ indicates the triggering of FTP function and vice versa)

$$T_{\mathrm{tri}}=\begin{cases} 0 & |\Delta f|\le F_{\mathrm{act}}\ \text{and}\ |R|\le R_{\mathrm{act}} \\ 1 & |\Delta f|>F_{\mathrm{act}}\ \text{or}\ |R|>R_{\mathrm{act}} \end{cases} \tag{28}$$

It is noted that F_{act} and R_{act} should be determined according to the local grid requirement for starting the frequency control function, which is coherent with the dead-zone range in the utility grid frequency regulation. The system frequency with indicators within F_{act} and R_{act} has high stability and quality, and no frequency control is required. When the indicators exceed F_{act} and R_{act}, the frequency control function (e.g., the proposed FTP block in this manuscript) should be activated to assure a better frequency performance.

In the analysis hereinafter, consider the case of sudden power shortage, i.e. $f_0=f_{\mathrm{N}}$, $P_{\mathrm{dis}}>0$. Based on the action parameters F_{act} and R_{act}, planning parameters F_{tp} and R_{tp}, and standard parameters F_{std} and R_{std}, three boundary lines, encompassing an FTP action line, an FTP planning line, and a grid code standard line are formed in the system frequency trajectory region, dividing the plane into 4 areas (see Fig. 5):

1) Safety area ($|\Delta f|<F_{act}$ and $|R|<R_{act}$): In this area, the system frequency deviation and RoCoF are insignificant, and the frequency stability is retained. As an explanatory example, f_1 and R_1 in Fig. 5 are always located in the safety area, indicating a small power disturbance, or ample intrinsic inertia-damping effect of the system to constrain its frequency trajectory. In this case, the droop-mode operation suffices the system stability, and it is not needed to provide additional inertia-damping effect. As a matter of fact, since the system mainly encounters small disturbances that can be managed by its intrinsic inertia-damping effect, the frequency mostly operates in this area.

2) Supervision area ($F_{act}<|\Delta f|<F_{tp}$ or $R_{act}<|R|<R_{tp}$): With the further increase of the disturbance level, the frequency trajectory crosses the safety area and enters the supervision area, and subsequently retains in this area (see f_2 and R_2 in Fig. 5) or goes beyond (see f_3 and R_3 in Fig. 5). Obviously, the system faces greater risk in the latter case, making it necessary to determine the safety of system frequency trajectory in advance and take corresponding actions. To this end, the real-time frequency trajectory f is continuously compared with the planned trajectory f_{TP}. If f is consistently within the region enclosed by f_{TP}, the droop-mode operation is maintained; otherwise further measures will

$$\begin{cases} |P_{\text{damper}}|_{\max} = K_{\text{p}} \lim\limits_{t\to\infty} |f_{\text{TP}} - f_{\text{FTP}}| = K_{\text{p}} \lim\limits_{t\to\infty} |(f_{\text{N}} - f_{\text{FTP}}) - (f_{\text{N}} - f_{\text{TP}})| \\ \qquad\qquad = K_{\text{p}} \lim\limits_{t\to\infty} |\Delta f_{\text{FTP}} - \Delta f_{\text{TP}}| = K_{\text{p}} \left(\lim\limits_{t\to\infty} |\Delta f_{\text{FTP}}| - \lim\limits_{t\to\infty} |\Delta f_{\text{TP}}| \right) \\ |P_{\text{inertia}}|_{\max} = K_{\text{d}} \lim\limits_{t\to t_0} |R_{\text{TP}} - R_{\text{FTP}}| = K_{\text{d}} \left(\lim\limits_{t\to t_0} |R_{\text{FTP}}| - \lim\limits_{t\to t_0} |R_{\text{TP}}| \right) \end{cases} \tag{31}$$

be taken, as discussed below.

3) Regulation area ($F_{tp} < |\Delta f| < F_{std}$ or $R_{tp} < |R| < R_{std}$): Frequency trajectory exceeding f_{TP} in the supervision area will eventually enter the regulation area, and may even reach the forbidden area. Since frequency in the regulation area indicates an acceptable (trigger thresholds F_{std} and R_{std} of frequency relays have not been reached) yet less safe (margins F_{mar} and R_{mar} are partially consumed) condition, the FTP function is triggered to provide additional inertia and damping support to the system, thereby reducing the consumption of safety margins. To this end, the PD controller immediately generates the power reference P_{TP} for frequency control that regulates the maximum values of frequency deviation and RoCoF toward the planned values F_{tp} and R_{tp}. Otherwise, if no additional inertia or damping support is provided, f will unavoidably enter the forbidden area.

4) Forbidden area ($|\Delta f| > F_{std}$ or $|R| > R_{std}$): Based on the previous analysis, frequency related relays will be triggered and a power outage is inevitable in this case (see f_3 and R_3 in Fig. 5). Hence, for a large disturbance that can cause frequency instability with the system intrinsic inertia-damping effect, sufficient support must be additionally provided in time, as such lowering the probability of triggering relevant protections and enhancing the system frequency stability. With the proposed FTP based strategy, the frequency trajectory can be effectively improved (e.g. from f_3 to f_{FTP} in Fig. 5) to guarantee the satisfaction of

$$\begin{cases} |\Delta f_{\text{FTP}}|_{\max} = \lim\limits_{t\to\infty} |\Delta f_{\text{FTP}}| < F_{\text{std}} \\ |R_{\text{FTP}}|_{\max} = \lim\limits_{t\to t_0} |R_{\text{FTP}}| < R_{\text{std}} \end{cases} \tag{29}$$

D. FTP Control Parameter Design

The FTP control is enabled by properly designed frequency deviation and RoCoF thresholds. It improves the frequency response and prevents f_{FTP} and R_{FTP} from entering the forbidden area by providing additional frequency regulation power P_{FTP} to the system. According to the auxiliary control strategy in Fig. 3, the frequency control power from the inverter is determined simultaneously by the inverter damping power P_{damper} and inertia power P_{inertia}, yielding

$$\begin{aligned} P_{\text{FTP}} &= P_{\text{damper}} + P_{\text{inertia}} \\ &= K_{\text{p}} \left(f_{\text{TP}} - f_{\text{FTP}} \right) + K_{\text{d}} \left(R_{\text{TP}} - R_{\text{FTP}} \right) \end{aligned} \tag{30}$$

From (23) and the frequency trajectory curves shown in Fig. 5, the difference between the system frequency under FTP control f_{FTP} and the planned frequency f_{TP} reaches the maximum value at the end of time, whereas the maximum difference between system RoCoF R_{FTP} and the RoCoF of planned trajectory R_{TP} is reached at the trigger time of FTP control, t_0. Accordingly, the maxima of the inverter damping power P_{damper} and inertia power P_{inertia} can be obtained as (31) shown at the top of this page.

By substituting (21), (23), and (29) into (31), we have

$$\begin{cases} |P_{\text{damper}}|_{\max} < K_{\text{p}} F_{\text{mar}} \\ |P_{\text{inertia}}|_{\max} < K_{\text{d}} R_{\text{mar}} \end{cases} \tag{32}$$

It is seen from (30) that larger controller parameters K_{p} and K_{d} result in greater P_{FTP}, and accordingly stronger additional inertia and damping effect. Consequently, the system frequency trajectory is closer to the planned one, and the frequency stability margins F_{mar} and R_{mar} are more sufficient. However, large frequency regulation power from the inverter can cause serious overload issues. Therefore, the frequency regulation power command P_{FTP} generated by the PD controller should be within the power limit of the inverter, i.e., $0 < P < P_{\max}$ (with $P_{\max}$ being the maximum inverter power).

According to the control scheme in Fig. 3, if the FTP control is enabled, the actual output power of the inverter yields

$$P = P_{\text{ref}} + P_{\text{FTP}} \tag{33}$$

Considering the inverter power constraint, and

$$-|P_{\text{FTP}}|_{\max} \le P_{\text{FTP}} \le |P_{\text{FTP}}|_{\max} \tag{34}$$

we have

$$\begin{cases} P_{\text{ref}} + |P_{\text{FTP}}|_{\max} \le P_{\max} \\ P_{\text{ref}} - |P_{\text{FTP}}|_{\max} \ge 0 \end{cases} \tag{35}$$

Consequently,

$$|P_{\text{FTP}}|_{\max} \le \min \left\{ P_{\text{ref}}, (P_{\max} - P_{\text{ref}}) \right\} \tag{36}$$

Besides, combination of (23), (30), and (31) indicates that at the moment of FTP triggering, P_{inertia} reaches the maximum value while P_{damper} is nearly naught, whereas the opposite holds at the end time. Hence, the maximum value of the absolute frequency regulation power is expressed as

$$|P_{\text{FTP}}|_{\max} = \begin{cases} |P_{\text{damper}}|_{\max} & |P_{\text{inertia}}|_{\max} \le |P_{\text{damper}}|_{\max} \\ |P_{\text{inertia}}|_{\max} & |P_{\text{inertia}}|_{\max} > |P_{\text{damper}}|_{\max} \end{cases} \tag{37}$$

Substituting (32) and (37) into (36) gives the PD parameter range of the FTP control, as

$$\begin{cases} K_{\text{p}} \le \dfrac{\min \left\{ P_{\text{ref}}, (P_{\max} - P_{\text{ref}}) \right\}}{F_{\text{mar}}} \\ K_{\text{d}} \le \dfrac{\min \left\{ P_{\text{ref}}, (P_{\max} - P_{\text{ref}}) \right\}}{R_{\text{mar}}} \end{cases} \tag{38}$$

For the droop-mode control used other than large disturbance cases, its parameter (droop coefficient D_{f}) can be designed according to the normal operating condition. The detailed process is omitted here for brevity.

IV. Verification of Proposed FTP Strategy

To prove the effectiveness and advancement of the proposed FTP based control strategy, in this Section, hardware-in-the-loop (HIL)-based experiments are first conducted in an ISPS with weak intrinsic inertia. The system topology is shown in Fig. 3, with detailed circuit and control parameters listed in Table I. Different scenarios of disturbances are considered, and the performance of the proposed control is compared versus that of the droop control and the VSG control. Then, the IEEE four-machine two-area (4M2A) system is adopted to verify the applicability and superiority of the proposed scheme in the complex multiple generation-unit (GU) system [17].

TABLE I
Main Parameters of the Test System.

Parameter	Value	Parameter	Value
V_N	380 V	Z_l	0.01 Ω / 0.2 mH
f_N	50 Hz	L_f	2.3 mH
P_{ref}	20 kW	P_L	20 kW
F_{std}	0.5 Hz	R_{std}	3.0 Hz/s
F_{tp}	0.4 Hz	R_{tp}	1.5 Hz/s
F_{act}	0.2 Hz	R_{act}	1.2 Hz/s
D_f	6700	T_f	130
D_V	8300	J_V	400
K_p	2×10^5	K_d	2500

A. Experiment scenario 1: consecutive small disturbances

In this scenario, the ISPS undergoes two subsequent small disturbances in the opposite direction, namely, the load power first suddenly reduces by 0.4 kW, followed by an increase of 0.8 kW. The results of system frequency are shown in Fig. 6. Both the droop control and VSG control can maintain system frequency stability by limiting the frequency deviation and RoCoF within the pertinent relay thresholds (0.2 Hz and 1.2 Hz/s). Specifically, with the additional inertia and damping support, the VSG control limits the maximum frequency deviation and maximum RoCoF to lower values (0.046 Hz and 0.45 Hz/s) w.r.t. the droop control (0.06 Hz and 0.8 Hz/s). Besides, the system frequency with the proposed FTP control is consistent with that adopting the droop control, indicating an effective mode selection by the proposed logic.

Though the effect of small disturbances can be mitigated by either control strategy here studied, it is worth mentioning that the droop control is usually preferred to avoid the potential oscillation issue. Moreover, since the small disturbance condition is a widely encountered case during practical operation, the droop control is the most commonly adopted strategy in standalone power systems.

B. Experiment scenario 2: consecutive large disturbances

In this case, the ISPS suffers from two large disturbances in the opposite direction, i.e. a load shedding of 4.0 kW followed by a sudden load increase of 9 kW. The results of system frequency are shown in Fig. 7. In this case, the maximum frequency deviation and RoCoF values of the ISPS reach 0.74 Hz and 9 Hz/s, respectively, exceeding the action thresholds of pertinent relays. To assure frequency stability, the VSG control is used to provide additional inertia and damping support to the system. Under the effect of the first disturbance, the maximum frequency deviation and RoCoF can be reduced to 0.48 Hz and 2.3 Hz/s respectively, which are lower than the relay thresholds. Though the VSG control is efficient also under the second disturbance (where the maximum frequency deviation and RoCoF are reduced to 0.58 Hz and 4.9 Hz/s respectively), it fails to limit frequency indicators within the safety region due to the doubled disturbance amplitude.

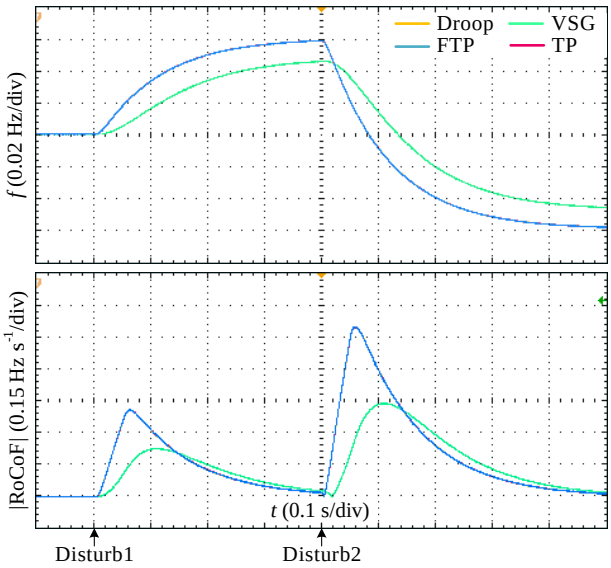

Fig. 6. Frequency responses of the ISPS with consecutive small disturbances.

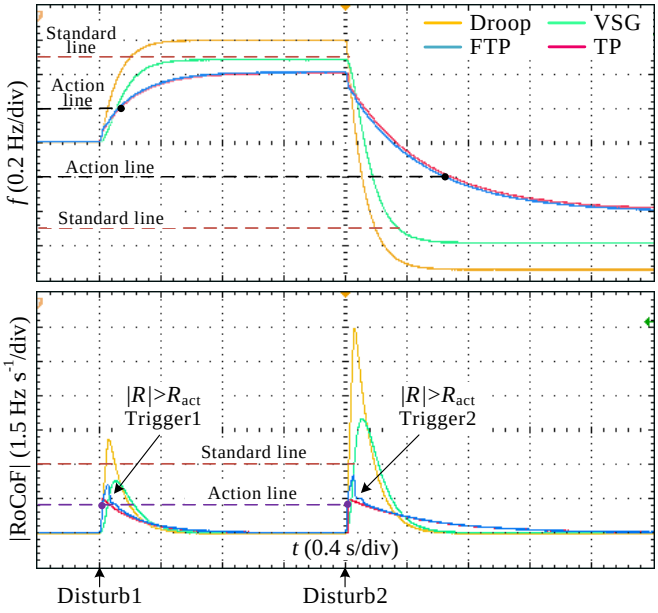

Fig. 7. Frequency responses of the ISPS with consecutive large disturbances.

When the proposed strategy is adopted, the system initially retains droop mode before frequency indicators become significant. During disturbances, the system RoCoF will first reach

its action threshold R_{act} (1.2 Hz/s) defined by the FTP control (see intersections denoted by purple dots) and trigger the FTP function. The control system subsequently plans a frequency trajectory (red curve) that meets the grid code requirement, and promptly provides necessary inertia and damping support to the system under the effect of PD control by regulating the system frequency trajectory (blue curve) toward the planned one. After a while, the frequency deviation also reaches its pertinent action threshold of FTP control, F_{act} (see intersections denoted by black dots); however, since sign(R) is unchanged, it is unnecessary to re-plan the frequency trajectory. These experiment results prove the ability of the FTP control to maintain frequency stability under large disturbances.

C. Experiment scenario 3: consecutive mixed disturbances

In this scenario, disturbances of different types are subsequently imposed. Specifically, the load power is i) firstly reduced by 1 kW, ii) reduced again by 3.5 kW and finally iii) increased by 9 kW.

With both the droop control and VSG control, the system frequency deviation and RoCoF are positively correlated with the disturbance level (see Fig. 8). Hence, these strategies cannot guarantee frequency stability in the event of a large disturbance. Specifically, when the droop control is adopted, the system can withstand the first impact, yet fails to meet the frequency indicator constraints during the subsequent disturbances [see the orange curves in Fig. 8(a)]. When the VSG control is used, the frequency performance is further improved; however, the frequency deviation under the second disturbance, and both frequency indicators under the third disturbance still fail the grid code requirement [see the green curves in Fig. 8(a)].

When the FTP based control strategy is adopted, frequency stability of the studied ISPS is significantly improved by closely tracking the planned trajectory. Specifically, the system intrinsic inertia and damping are sufficient under the first disturbance, where the maximum frequency deviation (0.14 Hz) and RoCoF (1.05 Hz/s) are marginally smaller than the action thresholds of the FTP control, and the inverter retains droop-mode operation. Under the effect of second disturbance, the system frequency deviation firstly reaches its action threshold F_{act} [see the blue curves in Fig. 8(b)], enabling the FTP function and planning the reference trajectory (see the red curves). By regulating the system frequency (see the blue curves) via the PD control, effective inertia and damping support is timely provided to the system. Due to the substantial disturbance level, the RoCoF also reaches its action threshold R_{act} during the control process, where the planned frequency trajectory is unchanged due to the consistent sign(R) value. Subsequently, for the third disturbance with drastic load power change, the FTP control process is activated by the RoCoF indicator, as shown in Fig. 8(c).

Besides, since the FTP based strategy is directly oriented by the desired frequency performance indicators, the inertia and damping of the ISPS are always guaranteed. Indeed, with the proposed strategy, the maxima of the system frequency deviation and RoCoF are virtually unaffected by the disturbance. This is one of the main advantages of the proposed method.

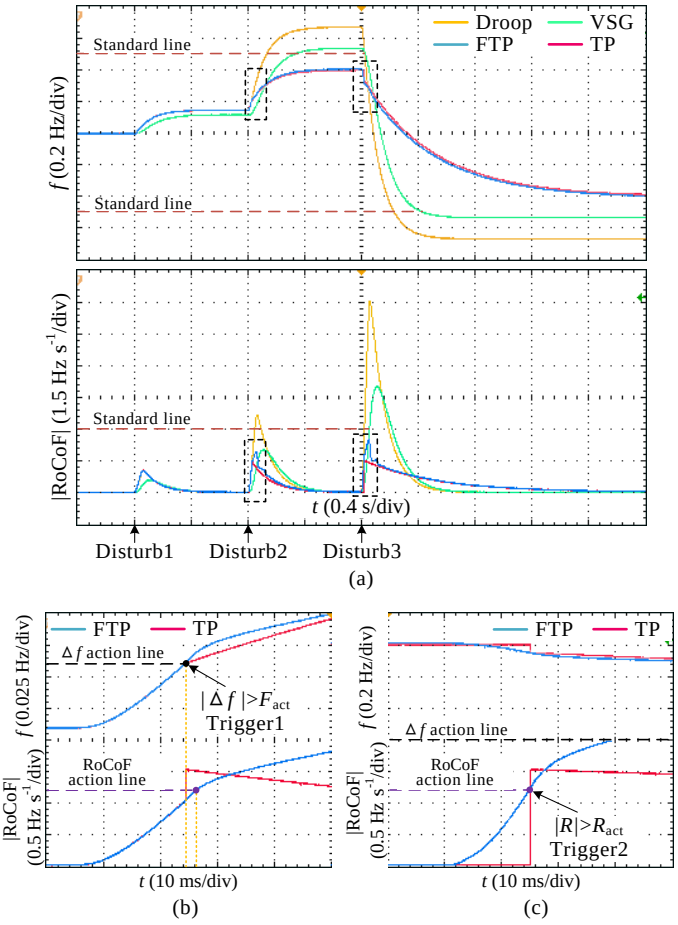

Fig. 8. Results of the ISPS with consecutive mixed disturbances: (a) frequency response, (b) FTP enabled by frequency deviation for the second disturbance, and (c) FTP enabled by RoCoF for the third disturbance.

D. Simulation of multi-GU system

With reference to Fig. 9, the 4th GU of the studied 4M2A system is replaced by two parallel inverters with capacities of 200 MW (#1) and 100 MW (#2), respectively, in order to validate the power sharing performance between the parallel inverters. To avoid the transient control strategy affecting the steady-state operation, all strategies are designed to assure the consistent steady-state inverter output power. The detailed parameters are listed in Table II. Since the IEEE 4M2A system has stronger inertia and damping owing to the SGs inside (GU1-GU3), the frequency stability issue is less severe than in the pure ISPS. Accordingly, more stringent frequency indicator requirements are adopted, with the aim to significantly improve the system frequency stability and quality.

The simulations are also divided into small- and large-disturbance scenarios. The load is suddenly decreased by 5 MW at 35 s for the small-disturbance condition and increased by 80 MW at 40 s for the large-disturbance condition. The results of system frequency [see Fig. 10(a)], RoCoF [see Fig. 10(b)], and output power of inverter #1 [see Fig. 10(c)] are compared. In the event of the large disturbance, the frequency deviation and RoCoF will sharply increase, even exceeding the relay thresholds. Therefore, it is critical for GUs to

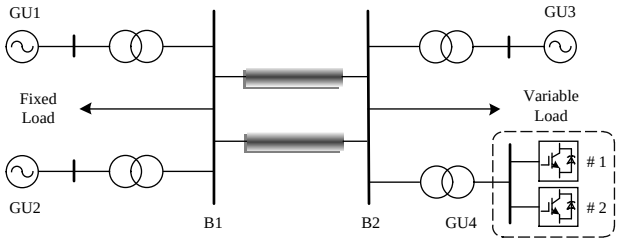

Fig. 9. Configuration of the studied IEEE 4M2A system.

TABLE II
MAIN PARAMETERS OF PARALLEL INVERTERS IN THE 4M2A SYSTEM.

	Parameter	Value	Parameter	Value
Frequency indicators	F_{std}	0.5 Hz	R_{std}	0.5 Hz/s
	F_{tp}	0.3 Hz	R_{tp}	0.3 Hz/s
	F_{act}	0.1 Hz	R_{act}	0.1 Hz/s
	Inverter #1		Inverter #2	
Droop control	P_{ref1}	100 MW	P_{ref2}	50 MW
	D_{f1}	5E7	D_{f2}	2.5E7
VSG control	J_{V1}	8E7	J_{V2}	4E7
	D_{V1}	6E7	D_{V2}	3E7
FTP control	K_{P1}	5E8	K_{P2}	2.5E8
	K_{D1}	1E8	K_{D2}	0.5E8

provide sufficient inertia and damping power, which are respectively proportional to the RoCoF and frequency deviation, to efficiently suppress these indicators during the transient caused by large disturbances. Besides, higher proportional gains contribute to increased emergency power provided by GUs, lower frequency deviation and RoCoF, and improved system frequency stability.

Based on the results, the inverter output power with the droop control is proportional to the system frequency deviation, regardless of the disturbance level. Accordingly, the droop control cannot provide the urgently needed inertia during the transient, nor provide more damping power accounting for the need to suppress the frequency deviation. Hence, the transient power support provided by the droop-controlled inverters is very limited, and the pertinent system has the worst behavior of frequency indicators (see the long dotted line in Fig. 10). The VSG control with an inertia unit provides pronounced inertia power support during the transient and sharply dropped the RoCoF indicator. However, constrained by the steady-state output power, the VSG-controlled inverters offer very limited damping power support and improvement in the frequency deviation (see the short dashed line Fig. 10). The poor damping performance also prevents the further inertia enhancement; indeed, as the inertia control parameter increases, the system oscillation is aggravated, and can easily lead to system instability. When the proposed strategy is adopted and the small disturbance condition is satisfied, the frequency indicators satisfy the relevant requirements, the FTP function is disabled, and the system frequency response is perfectly consistent with the droop-controlled system. Under the large disturbance condition, the inverter with the FTP control not only enhances the transient system damping capacity, but also

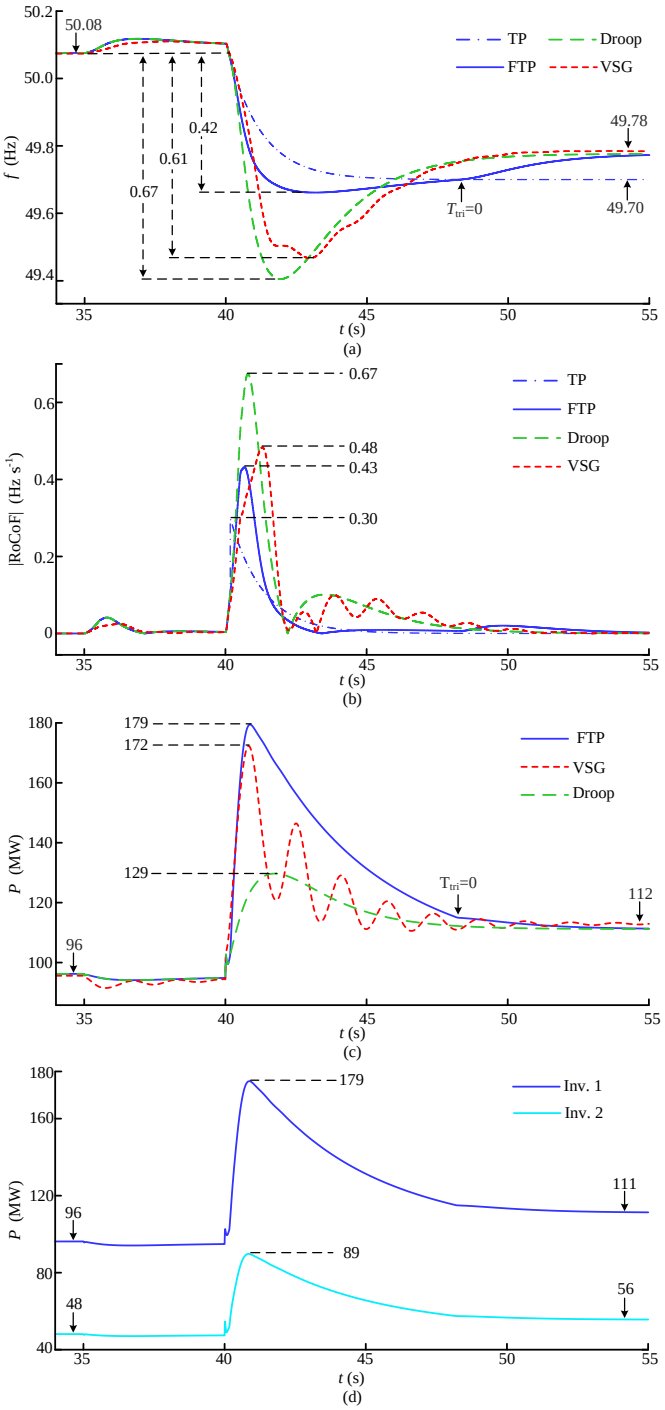

Fig. 10. 4M2A system dynamics with different frequency control schemes: (a) frequency, (b) absolute RoCoF, and (c) active power output by inverter #1 . (d) Output power profiles of inverters #1 and #2 with the FTP control.

provides inertia power support, thereby significantly limiting the system frequency deviation and RoCoF. Finally, it can automatically and smoothly return to the droop control mode, as shown in Fig. 10 (when $T_{tri} = 0$). Simulation results again prove the on-demand inertia/damping power support ability of the proposed strategy based on the system state, which does not affect the steady-state power flow of the system.

Besides, the FTP control can distribute power autonomously in line with the inverter capacity ratio. As shown in Fig.

10(d), the two inverters have a constant ratio of 2:1 for the output power, regardless of the operation condition (transient or steady-state).

V. Conclusion

Due to lack of inertia and damping support from the large power grid, standalone power systems usually have weak frequency stability. In this paper, an FTP based control strategy is proposed, aiming to ensure restrained frequency deviation and RoCoF indicators of the ISPS under various disturbance conditions. The main conclusions are:

1) When using the droop/VSG control, frequency deviation and RoCoF indicators of the system are positively correlated with the magnitude of disturbance. Limited by several technical issues, parameters of droop/VSG control can only be designed according to typical working conditions, yet fails to meet the operation requirement for ISPSs in the presence of large disturbances. In these cases, the frequency indicators are likely to exceed the safety thresholds and trigger pertinent relays.
2) The FTP control is an efficient inertia/damping support method directly oriented by frequency performance indicators. The system inertia and damping after control are always sufficient as long as planning parameters are suitably designed to be marginally smaller than the relays thresholds, thus avoiding the need to estimate the disturbance power and the system inertia/damping shortage. Frequency stability of the ISPS can be retained under complex disturbances.
3) The proposed FTP based strategy inherits the advantages of the droop control, meanwhile avoids the oscillation problem associated with the VSG control. It has excellent applicability to both grid-tied and standalone conditions. Experiments and simulations in various scenarios and with comprehensive disturbances proved the effectiveness and advancement of the proposed strategy in assuring system frequency stability.

References

[1] R. H. Lasseter, Z. Chen, and D. Pattabiraman, "Grid-forming inverters: A critical asset for the power grid," *IEEE J. Emerg. Sel. Top. Power Electron.*, vol. 8, no. 2, pp. 925–935, 2020.

[2] M. Huang, Y. Peng, C. Tse *et al.*, "Bifurcation and large signal stability analysis of three-phase voltage-source converters under grid voltage dips," *IEEE Trans. Power Electron.*, vol. 32, no. 11, pp. 8868–8879, 2017.

[3] L. Xiong, X. Liu, Y. Liu, and F. Zhuo, "Modeling and stability issues of voltage-source converter dominated power systems: A review," *CSEE J. Power Energy Syst.*, to be published, doi: 10.17775/CSEE-JPES.2020.03590.

[4] J. Fang, H. Li, Y. Tang, and F. Blaabjerg, "On the inertia of future more-electronics power systems," *IEEE J. Emerg. Sel. Top. Power Electron.*, vol. 7, no. 4, pp. 2130–2146, 2019.

[5] S. D'Arco and J. A. Suul, "Equivalence of virtual synchronous machines and frequency-droops for converter-based MicroGrids," *IEEE Trans. Smart Grid*, vol. 5, no. 1, pp. 394–395, 2014.

[6] R. Domínguez, A. J. Conejo, and M. Carrión, "Toward fully renewable electric energy systems," *IEEE Trans. Power Syst.*, vol. 30, no. 1, pp. 316–326, 2015.

[7] X. Meng, J. Liu, and Z. Liu, "A generalized droop control for grid-supporting inverter based on comparison between traditional droop control and virtual synchronous generator control," *IEEE Trans. Power Electron.*, vol. 34, no. 6, pp. 5416–5438, 2019.

[8] Q. Zhong and G. Weiss, "Synchronverters: Inverters that mimic synchronous generators," *IEEE Trans. Ind. Electron.*, vol. 58, no. 4, pp. 1259–1267, 2011.

[9] W. Zhang, D. Remon, and P. Rodriguez, "Frequency support characteristics of grid-interactive power converters based on the synchronous power controller," *IET Renew. Power Gener.*, vol. 11, no. 4, pp. 470–479, 2017.

[10] Y. Hirase, K. Sugimoto, K. Sakimoto, and T. Ise, "Analysis of resonance in microgrids and effects of system frequency stabilization using a virtual synchronous generator," *IEEE J. Emerg. Sel. Top. Power Electron.*, vol. 4, no. 4, pp. 1287–1298, 2016.

[11] J. Alipoor, Y. Miura, and T. Ise, "Power system stabilization using virtual synchronous generator with alternating moment of inertia," *IEEE J. Emerg. Sel. Top. Power Electron.*, vol. 3, no. 2, pp. 451–458, 2015.

[12] M. A. Torres L., L. A. C. Lopes, L. A. Morán T., and J. R. Espinoza C., "Self-tuning virtual synchronous machine: A control strategy for energy storage systems to support dynamic frequency control," *IEEE Trans. Energy Convers.*, vol. 29, no. 4, pp. 833–840, 2014.

[13] A. Karimi, Y. Khayat, M. Naderi *et al.*, "Inertia response improvement in AC microgrids: A fuzzy-based virtual synchronous generator control," *IEEE Trans. Power Electron.*, vol. 35, no. 4, pp. 4321–4331, 2020.

[14] D. Li, Q. Zhu, S. Lin, and X. Y. Bian, "A self-adaptive inertia and damping combination control of VSG to support frequency stability," *IEEE Trans. Energy Convers.*, vol. 32, no. 1, pp. 397–398, 2017.

[15] F. Wang, L. Zhang, X. Feng, and H. Guo, "An adaptive control strategy for virtual synchronous generator," *IEEE Trans. Ind. Appl.*, vol. 54, no. 5, pp. 5124–5133, 2018.

[16] J. Alipoor, Y. Miura, and T. Ise, "Stability assessment and optimization methods for microgrid with multiple VSG units," *IEEE Trans. Smart Grid*, vol. 9, no. 2, pp. 1462–1471, 2018.

[17] L. Xiong, X. Liu, D. Zhang, and Y. Liu, "Rapid power compensation based frequency response strategy for low inertia power systems," *IEEE J. Emerg. Sel. Top. Power Electron.*, to be published, doi: 10.1109/JESTPE.2020.3032063.

[18] J. Zhao, M. Huang, H. Yan *et al.*, "Nonlinear and transient stability analysis of phase-locked loops in grid-connected converters," *IEEE Trans. Power Electron.*, vol. 36, no. 1, pp. 1018–1029, 2021.